Supplementary Materials for Nanowire melting modes during the Solid-Liquid Phase Transition: Theory and Molecular Dynamics Simulations

KANNAN M. RIDINGS[1,2,*] AND SHAUN C. HENDY[3]

[1] *The University of Auckland, Department of Physics, Auckland, 1010, New Zealand*
[2] *Affiliation, department, city, postcode, country*
[3] *Toha Foundry, Auckland, 1025, New Zealand*

1. S1 INTRODUCTION

Supplementary information for the paper *Nanowire melting modes during the Solid-Liquid Phase Transition: Theory and Molecular Dynamics Simulations* is contained in this document. It includes details of the molecular dynamics (MD) simulations and the computational methodology used in the analysis of the MD simulations presented in the accompanying paper. Additionally, it features the same analysis used on the solid-liquid interface to the liquid interface. All atomistic visualisations were made with Ovito [1].

2. S2 COMPUTATIONAL DETAILS

FCC nanowires are bounded by {100} and {110} surfaces, which are made via a Wulff-type construction (see [2] Figure 2). This ensured that the initial state of each nanowire is bounded by the same surfaces, and have approximately the same proportion of atoms on the {100} surfaces to the {110} surfaces. This helps to rule out any differences in observations due to the presence of more (or less) atoms on one surface compared to another, which can lead to differences in surface energies.

To account for the expansion of the lattice, an atomic volume of approximately $V_{\text{atom}} = 13.2\text{Å}$ was used. This assumed the density of copper at the melting point was $\rho_{_{Cu}} = 8020\ \text{kg/m}^3$.

The phase of each atom was determined by modified Steinhardt parameters [3, 4]. Looking at Fig. S1 we see a bimodal distribution of $\overline{q_6}$, with one peak being found at $\overline{q_6} \approx 0.189$, and another at $\overline{q_6} \approx 0.417$. This helps define a threshold of $\overline{q_{cut}} \approx 0.300$, where if $\overline{q_6} > \overline{q_{cut}}$ the atom is more likely to be in a solid phase, and if $\overline{q_6} < \overline{q_{cut}}$ the atom is more likely to be in a liquid phase. We then use temporal averaging to reassign potential 'misclassified' atoms. We look at atoms at a time t_i and t_{i+1}, and if atoms have switched phases from time t_i to time t_{i+1}, we reassign the atom the phase it had at time t_i. This clears up most misclassified atoms in the system.

To estimate values of the melting temperature, we calculated heat capacity $C_{\text{v}} = \frac{dE}{dT}$ and use the peak to identify the bulk melting temperature of each wire, where the C_{v} diverges $T \to T_{\text{m}}$. These were averaged across multiple runs for each wire to give a reliable estimate of the melting temperature for each wire.

3. S3 SUPPLEMENTARY MD DETAILS

This section contains additional information on the analysis of the MD simulations used to construct the arguments in the main manuscript. To study the interface stability, we averaged binned values of $r^*(z)$ along the wire axis prior to the solid pinch-off to obtain an estimate of $\bar{r^*}$. A nearest-neighbour algorithm is then used to extract atoms at the solid-liquid interface. Once all the atoms in the solid are appropriately classified, we can check how many neighbours each atom has within a range r_{cut}, where r_{cut} is generally chosen to be within the first or second nearest-neighbour shell. This can isolate most atoms at the interface to estimate the solid radius, r^*, at a point along the wire axis. The atoms at the solid-liquid interface are then binned along the axis of each wire so that an estimate of $r^*(z)$ can be obtained. Once $r^*(z)$ is calculated, we can

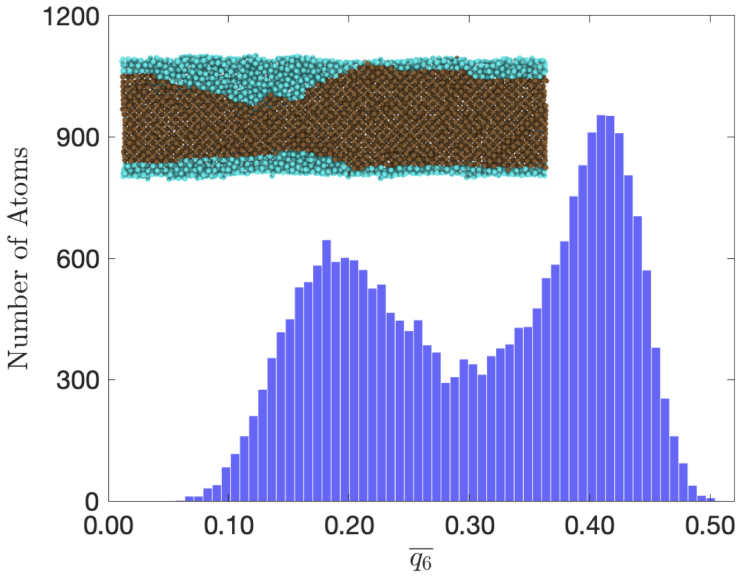

Fig. S1. This figure shows the bimodal distribution of the $\overline{q_6}$ order parameter during the solid-liquid phase transition with an accompanying snapshot.

compute the Fourier transform of the interface profile. When calculating the Fourier transform of a given interface, a sampling frequency $f_s = 4$ was chosen since this was the nearest whole number to the lattice spacing of copper that was used in this study. In Fig. S2), the distance between the top layer of the interface profile and the bottom layer is approximately 4, justifying our choice of sampling frequency.

The Fourier transform of $r^*(z)$ was taken to extract modes that destabilised the solid-liquid interface. Destabilising modes of k_{sol} (k_{max} for the solid-liquid interface) were averaged across all runs, giving a more reliable estimate of the Fourier profile for each wire. Fig. S3 shows the Fourier transform for wires of initial radii $R_0 = 38$, 30, 22 Å, with each satisfying $L/R_0 = 25$. This is obtained by taking the Fourier transform of the solid profile, seen in Figure 3 of the main text. The Fourier transform for each wire is taken across multiple MD runs, and averaged to extract values of k_{sol} (k_{max} for the solid-liquid interface), which can be seen in Figure 4 of the main text.

Fig. S4 shows the interface profile of a liquid nanowire of length $L = 1084$ Å as it begins to break up. The interface profile is smooth due to the presence of higher surface tension (when compared to the solid-liquid interface). The necking of the wire is caused by the atoms in the neck migrating away to increase their coordination number.

In Fig. S5 we see the Fourier transform for a wire of radius $R_0 \approx 30$ Å and length $L = 1084$ Å, which is calculated by taking the average of 25 individual MD runs. This shows a distinct mode destabilising the liquid interface. This can particularly be seen when we compare it to Fig. S3, where modes that destabilise the solid-liquid interface appear to be proportional to the wire length.

Next, we see Fig. S6, the stability diagram for the liquid in terms of the fastest growing modes $k_{liq}R_0$ (where k_{liq} is k_{max} for the liquid) against the wire aspect ratio L/R_0. In the case of the liquid, wires shorter than a critical length (where $L_{crit} \simeq 2\pi R_0$), the breakup of the liquid interface will not happen.

PR theory predicts that $k_{max}R_0 \approx 0.697$ (or $\lambda \approx 9.01R_0$). Fig. S6 suggests that at the nanoscale, this number is lower, where it is found that $k_{liq}R_0 \approx 0.423$ (giving $lambda \approx 14.85R_0$). This is slightly higher than what has been reported previously [5], but consistent with the result that PR theory over predicts the fastest growing modes at the nanoscale [6].

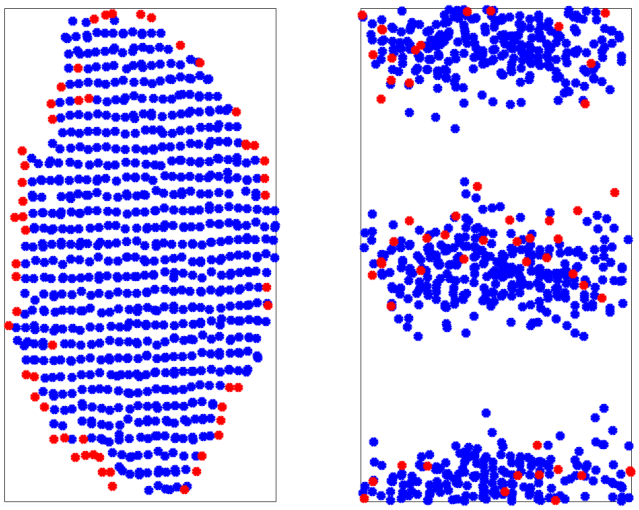

Fig. S2. This is an example of how the solid radius, r^* is defined. On the left is a slice of the xy-plane for one sampling of the interface, and on the right is the view down the xz-plane. The red points are used to approximate $r^*(z)$ by averaging over all the points in that segment of the wire.

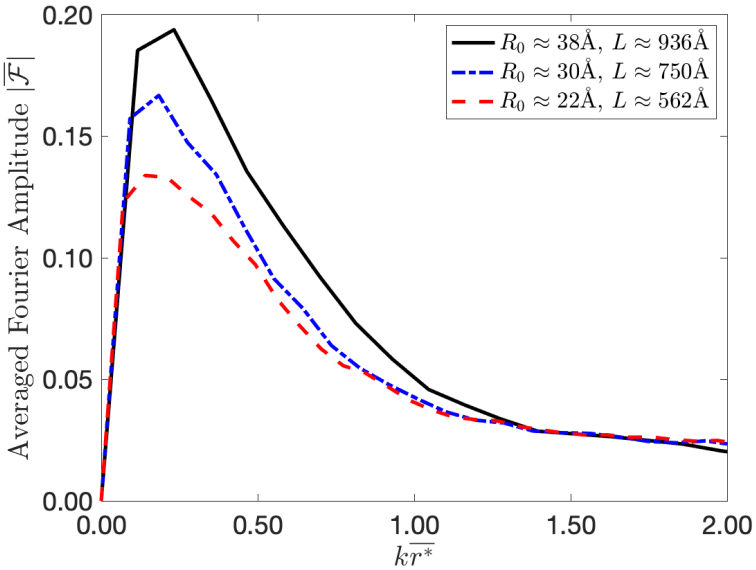

Fig. S3. The averaged Fourier transform of wires with $L/R_0 = 25$. Values of k_{sol} for each wire are all low, indicating modes that destabilise the solid-liquid interface are proportional to the wire length.

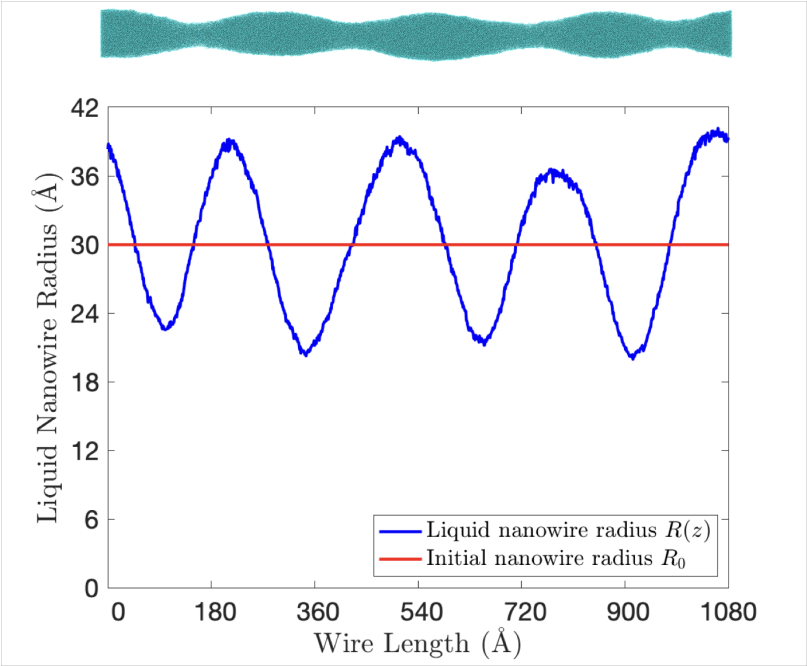

Fig. S4. A single MD run showing how the liquid nanowire radius $R(z)$ varies across its length, with an accompanying snapshot. Marked in red is the initial wire radius R_0. The interface profile here is smooth, with the undulations in the wire clearly represented when compared to the snapshot.

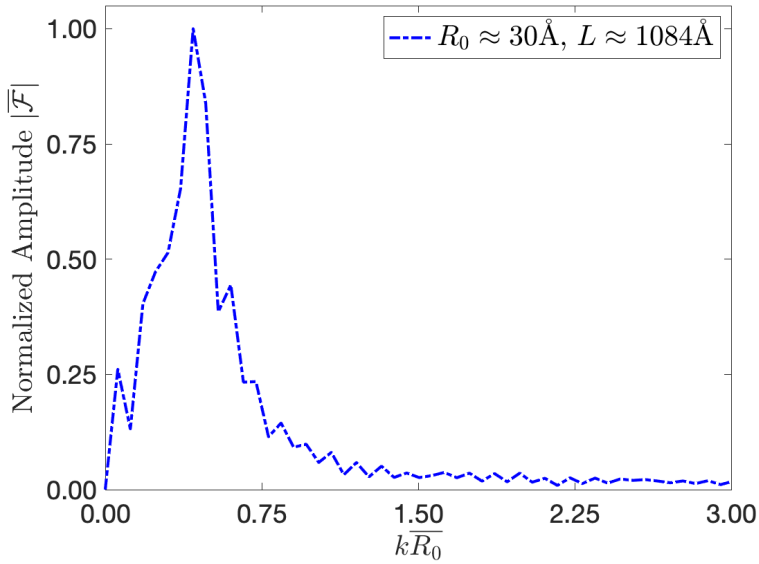

Fig. S5. The Fourier transform of the liquid interface profile has been calculated for 25 individual MD runs, and is averaged across all simulations. A clear distinct mode can be seen giving a value of $k_{liq}R_0 \approx 0.421$.

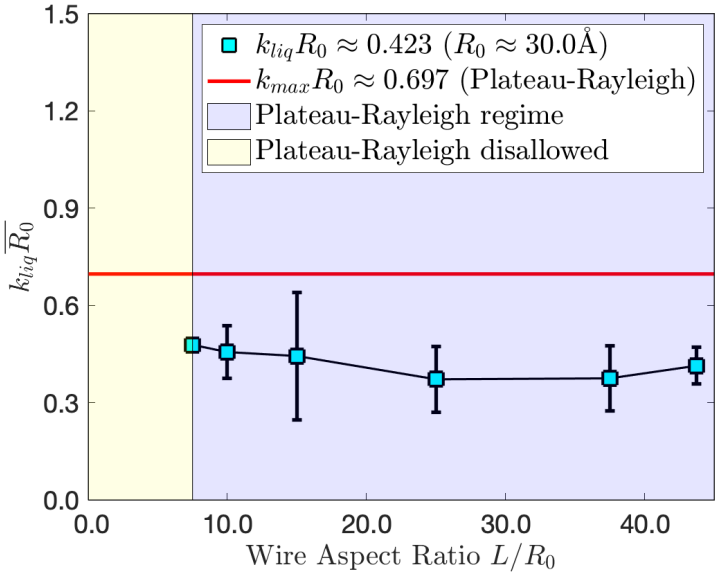

Fig. S6. This figure shows how modes that destabilise the liquid interface change with the wire aspect ratio. As we can see, the relationship is approximately flat, showing that $k_{liq}R_0 \approx 0.423$ for a liquid nanowire. The blue shaded region shows where liquid wires are unstable to perturbations, and the yellow shaded region shows where the PR breakup of the interface is disallowed.

REFERENCES

1. A. Stukowski, "Visualization and analysis of atomistic simulation data with ovito–the open visualization tool," Model. simulation materials science engineering **18**, 015012 (2009).
2. K. M. Ridings, T. S. Aldershof, and S. C. Hendy, "Surface melting and breakup of metal nanowires: Theory and molecular dynamics simulation," The J. chemical physics **150**, 094705 (2019).
3. P. J. Steinhardt, D. R. Nelson, and M. Ronchetti, "Bond-orientational order in liquids and glasses," Phys. Rev. B **28**, 784 (1983).
4. W. Lechner and C. Dellago, "Accurate determination of crystal structures based on averaged local bond order parameters," The J. chemical physics **129**, 114707 (2008).
5. J. Eggers and T. F. Dupont, "Drop formation in a one-dimensional approximation of the navier–stokes equation," J. fluid mechanics **262**, 205–221 (1994).
6. C. Zhao, J. E. Sprittles, and D. A. Lockerby, "Revisiting the rayleigh–plateau instability for the nanoscale," J. Fluid Mech. **861** (2019).